

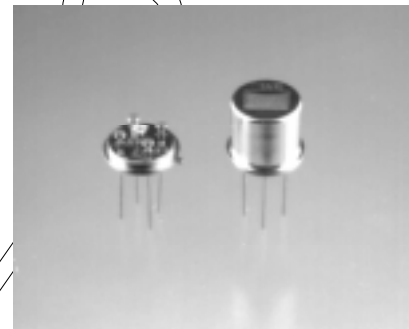
FIGARO

an ISO9001 company



**Technical Information for Air Quality Control Sensors**

The Figaro 2600 series is a new type thick film metal oxide semiconductor, screen printed gas sensor which offers miniaturization and lower power consumption. The TGS2600 displays high selectivity and sensitivity to low concentrations of various air contaminants such as those found in cigarette smoke.



	<u>Page</u>
<i>Specifications</i>	
<b>Features</b> .....	2
<b>Applications</b> .....	2
<b>Structure</b> .....	2
<b>Basic measuring circuit</b> .....	2
<b>Circuit &amp; operating conditions</b> .....	3
<b>Specifications</b> .....	3
<b>Dimensions</b> .....	3
<i>Basic Sensitivity Characteristics</i>	
<b>Sensitivity to various gases</b> .....	4
<b>Temperature and humidity dependency</b> .....	5-6
<b>Heater voltage dependency</b> .....	6
<b>Gas response</b> .....	7
<b>Initial action</b> .....	8
<b>Long term characteristics</b> .....	8-9

See also Technical Brochure 'Technical Information on Usage of TGS Sensors for Toxic and Explosive Gas Leak Detectors'.

**IMPORTANT NOTE:** OPERATING CONDITIONS IN WHICH FIGARO SENSORS ARE USED WILL VARY WITH EACH CUSTOMER'S SPECIFIC APPLICATIONS. FIGARO STRONGLY RECOMMENDS CONSULTING OUR TECHNICAL STAFF BEFORE DEPLOYING FIGARO SENSORS IN YOUR APPLICATION AND, IN PARTICULAR, WHEN CUSTOMER'S TARGET GASES ARE NOT LISTED HEREIN. FIGARO CANNOT ASSUME ANY RESPONSIBILITY FOR ANY USE OF ITS SENSORS IN A PRODUCT OR APPLICATION FOR WHICH SENSOR HAS NOT BEEN SPECIFICALLY TESTED BY FIGARO.

1. Specifications

1-1 Features

- \* High selectivity to low gas concentrations
- \* Low power consumption
- \* Small size
- \* Long life

1-2 Applications

- \* Air cleaners for indoor air cleaners
- \* Air cleaners for vehicles
- \* Air quality monitors

1-3 Structure

Figure 1 shows the structure of TGS2600. Using thick film techniques, the sensor material is printed on electrodes (Au) which have been printed onto an alumina substrate. The main sensing material of the sensor element is tin dioxide (SnO<sub>2</sub>). One electrode is connected to pin No.2 and the other is connected to pin No.3. An RuO<sub>2</sub> heater printed onto the reverse side of the substrate and connected to pins No.1 and No.4 heats the sensing material.

Lead wires are Pt-W 8% of 0.04mm diameter and are spot welded to sensor pins which are made of Ni-plated Ni-Fe 50%.

The sensor base is made of Ni-plated steel. The sensor cap is made of a NiCu-plated steel (JIS,SPCC-SB). The upper opening in the cap is covered with a double layer of 100 mesh stainless steel gauze (SUS316).

1-4 Basic measuring circuit

Figure 2 shows the basic measuring circuit. Circuit voltage (V<sub>c</sub>) is applied across the sensor element which has a resistance (R<sub>s</sub>) between the sensor's two electrodes and the load resistor (R<sub>L</sub>) connected in series. DC voltage is always required for the circuit voltage. The sensor signal (V<sub>RL</sub>) is measured indirectly as a change in voltage across the R<sub>L</sub>. The R<sub>s</sub> is obtained from the formula shown at the right.

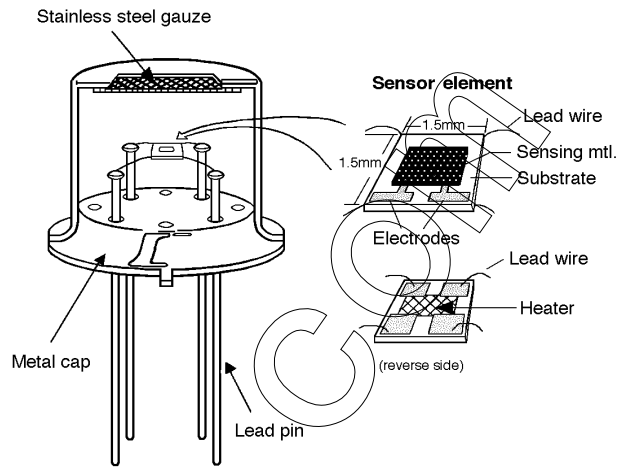


Fig. 1 - Sensor structure

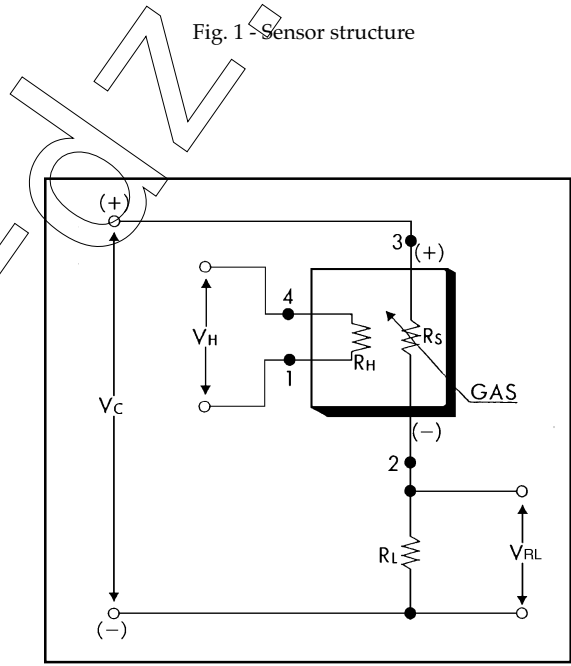


Fig. 2 - Basic measuring circuit

$$R_s = \frac{V_c - V_{out}}{V_{out}} \times R_L$$

Formula to determine R<sub>s</sub>

## 1-5 Circuit & operating conditions

The ratings shown below should be maintained at all times to insure stable sensor performance:

Item	Specification
Circuit voltage (Vc)	5.0V ± 0.2V DC
Heater voltage (VH)	5.0V ± 0.2V DC/AC
Heater resistance (room temp.)	80 ± 8Ω
Load resistance (RL)	Variable (min = Vc <sup>2</sup> /60)
Sensor power dissipation (Ps)	≤ 15mW
Operating & storage temperature	-10°C ~ +50°C
Optimal detection concentration	50 ~ 5,000ppm

## 1-6 Specifications NOTE 1

Item	Specification
Sensor resistance (air)	10kΩ ~ 90kΩ
Sensor resistance gradient (β)	0.3 ~ 0.6
$\beta = R_s(10\text{ppm hydrogen})/R_s(\text{air})$	
Heater current	42 ± 10mA
Heater power consumption	210 ± 25mW

### Mechanical Strength:

The sensor shall have no abnormal findings in its structure and shall satisfy the above electrical specifications after the following performance tests:

**Withdrawal Force** - withstand force > 5kg in each direction

**Vibration** - frequency-1000c/min., total amplitude-4mm, duration-one hour, direction-vertical

**Shock** - acceleration-100G, repeated 5 times

## 1-7 Dimensions

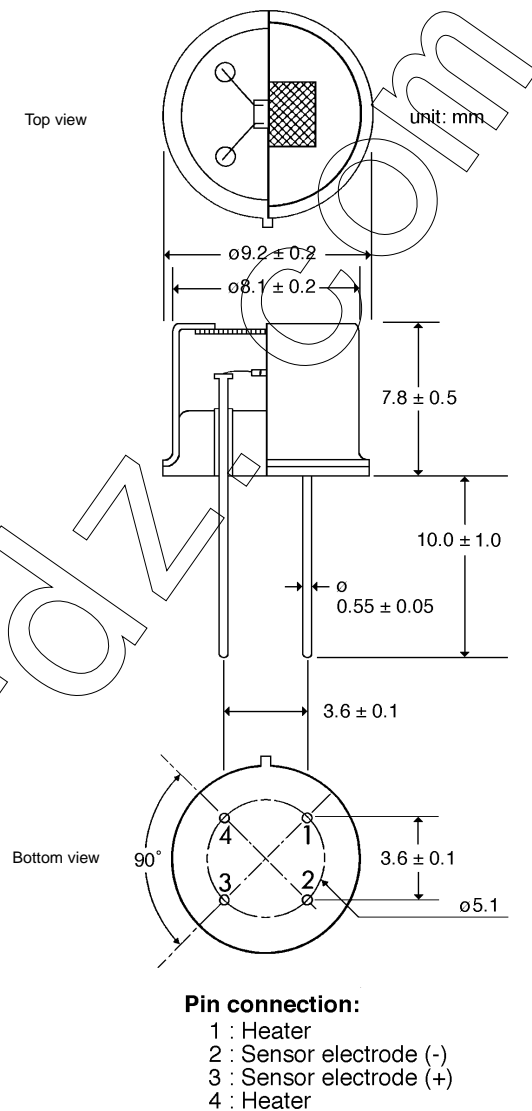


Fig. 3 - Sensor dimensions

**NOTE 1:** Sensitivity characteristics are obtained under the following standard test conditions:

(Standard test conditions)

Temperature and humidity: 20 ± 2°C, 65 ± 5% RH

Circuit conditions: Vc = 5.0 ± 0.05V DC

VH = 5.0 ± 0.05V DC

RL = 10.0kΩ ± 1%

Preheating period: 7 days or more under standard circuit conditions.

2. Basic Sensitivity Characteristics

2-1 Sensitivity to various gases

Figure 4 shows the relative sensitivity of TGS2600 to various gases. The Y-axis shows the ratio of the sensor resistance in various gases ( $R_s$ ) to the sensor resistance in clean air ( $R_o$ ) taken at standard test conditions of 20°C / 65%RH.

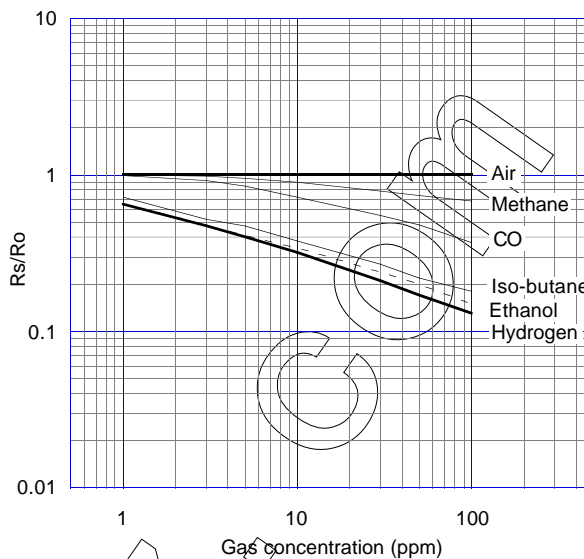


Fig. 4 - Sensitivity to various gases ( $R_s/R_o$ )

Figure 5 shows the relative sensitivity of TGS2600 to various gases in cigarette smoke. The Y-axis shows the ratio of the sensor resistance in cigarette smoke ( $R_s$ ) to the sensor resistance in clean air ( $R_o$ ) taken at standard test conditions of 20°C / 65%RH. This data was taken in a 20m<sup>3</sup> room with cigarettes placed on a flat surface. The burning time for one cigarette was approximately 8 minutes. (Note: Generally, the activation point for an air cleaner would be around  $R_s/R_o=0.85$ , while the  $R_s/R_o$  for just one cigarette is as low as 0.65, making this sensor ideal for air cleaner application).

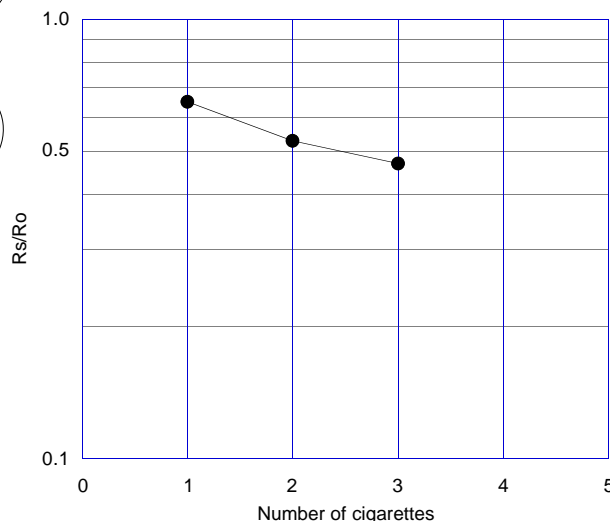


Fig. 5 - Sensitivity to cigarette smoke ( $R_s/R_o$ )

This data shows that TGS2600 has good sensitivity to low concentrations of air contaminants, including those found in cigarette smoke.

**NOTE:**

All sensor characteristics in this technical brochure represent typical sensor characteristics. For additional information on the usage of the sensor in air cleaners, please refer to.....

2-2 Temperature and humidity dependency

Figure 6 shows the temperature and humidity dependency of TGS2600 in clean air. The Y-axis shows the ratio of sensor resistance in clean air under various atmospheric conditions ( $R_s$ ) to the sensor resistance in clean air at 20°C / 65%RH ( $R_o$ ).

R.H. (°C)	40%R.H.	65%R.H.	85%R.H.	100%R.H.
-10				2.35
0				1.60
10	1.61	1.42	1.25	
20	1.30	1.00	.93	
30	.99	.80	.70	
40	.78	.61	.54	
50	.63	.48	.43	

Table 1 - Temperature and humidity dependency (typical values of  $R_s/R_o$  for Fig. 6)

Table 1 shows a table of values of the sensor's resistance ratio ( $R_s/R_o$ ) under the same conditions as those used to generate Figure 6.

Figure 7 shows the temperature and humidity dependency of TGS2600 in hydrogen. The Y-axis shows the ratio of sensor resistance in 10ppm of hydrogen under various atmospheric conditions ( $R_s$ ) to the sensor resistance in clean air under the same atmospheric conditions ( $R_o$ ).

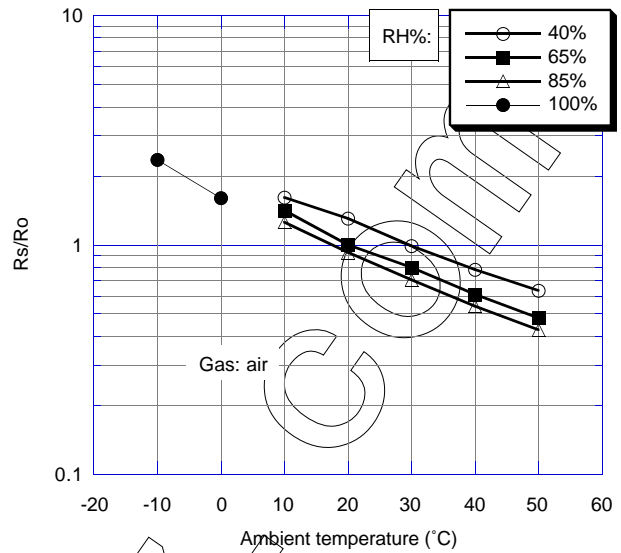


Fig. 6 - Temperature and humidity dependency ( $R_s/R_o$ ) in clean air

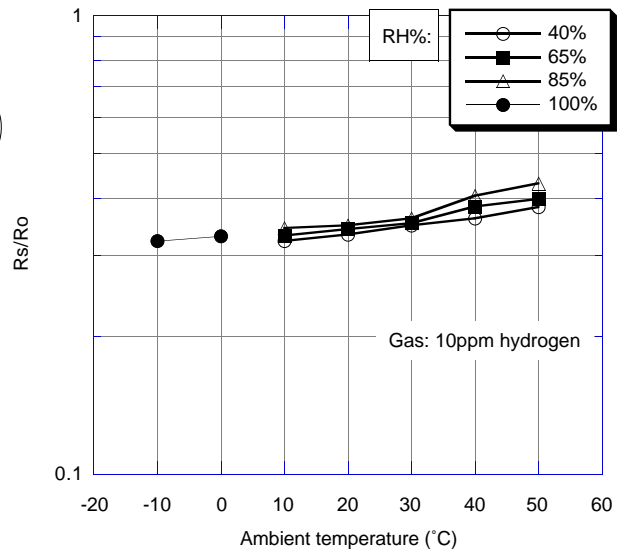


Fig. 7 - Temperature and humidity dependency ( $R_s/R_o$ ) in 10ppm of hydrogen

Figure 8 shows the temperature and humidity dependency of TGS2600 in ethanol (used as a representative gas for VOCs to which the sensor is likely to respond). The Y-axis shows the ratio of sensor resistance in 30ppm of ethanol under various atmospheric conditions ( $R_s$ ) to the sensor resistance in clean air under the same atmospheric conditions ( $R_o$ ).

This section demonstrates that, when used in the range of  $10^{\circ}\text{C}\sim 50^{\circ}\text{C}$ , sensitivity in air (Fig. 6) shows temperature dependency, but sensitivity in gas (Figs. 7 & 8) is relatively unaffected by temperature. As a result, temperature compensation for the sensor is not required, although if a greater accuracy is desired, temperature compensation for air values can be done.

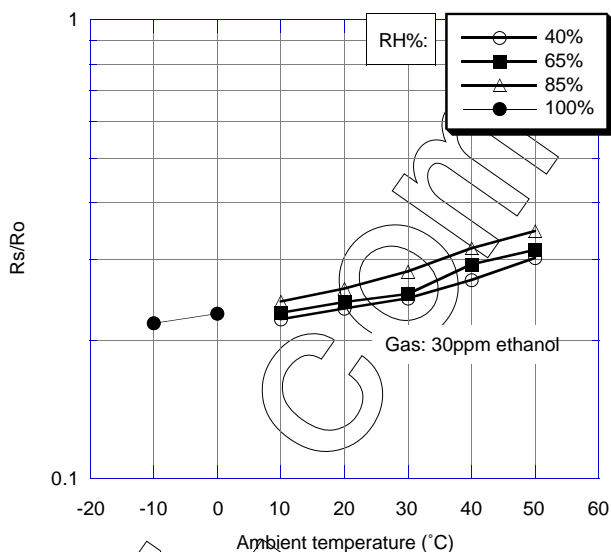


Fig. 8 - Temperature and humidity dependency ( $R_s/R_o$ ) in 30ppm of ethanol

### 2-3 Heater voltage dependency

Figure 9 shows the change of the sensor resistance ratio in clean air according to variations in the heater voltage ( $V_H$ ). The Y-axis shows the ratio of sensor resistance in clean air at various heater voltages ( $R_s$ ) compared to sensor resistance in clean air at  $V_H=5.0\text{V}$  ( $R_o$ ).

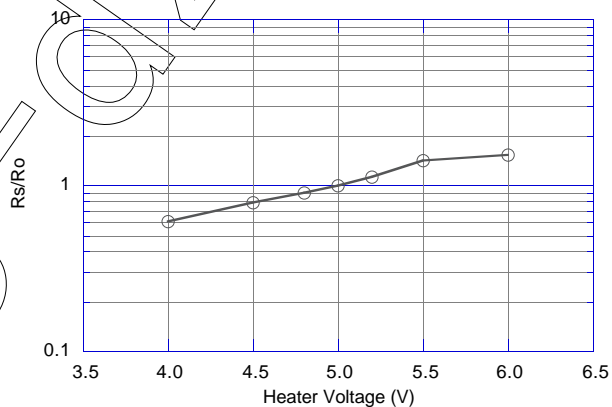


Fig. 9 - Heater voltage dependency in clean air

Figure 10 shows the change of the sensor resistance ratio in hydrogen and ethanol according to variations in the heater voltage ( $V_H$ ). The Y-axis shows the ratio of sensor resistance in gases at various heater voltages ( $R_s$ ) compared to sensor resistance in clean air at the same heater voltage ( $R_o$ ).

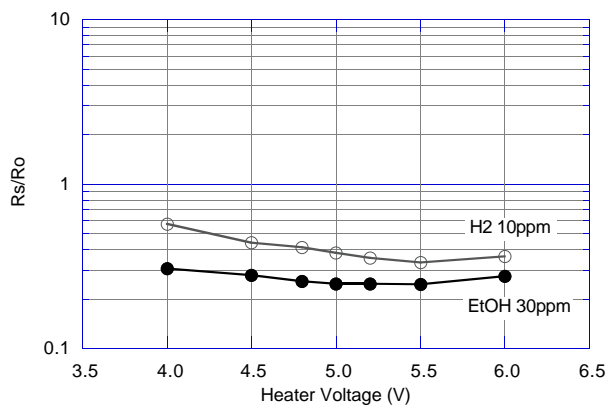


Fig. 10 - Heater voltage dependency in various gases

Note that 5.0V as a heater voltage must be maintained because variance in applied heater voltage will cause the sensor's characteristics to be changed from the typical characteristics shown in this brochure.

2-4 Gas response

Figure 11 shows the response pattern of the sensor when inserted into and later removed from 10ppm of hydrogen after a 3 minute period. The Y-axis shows the ratio of sensor resistance over time ( $R_s$ ) compared with sensor resistance in clean air just prior to insertion into hydrogen ( $R_o$ ).

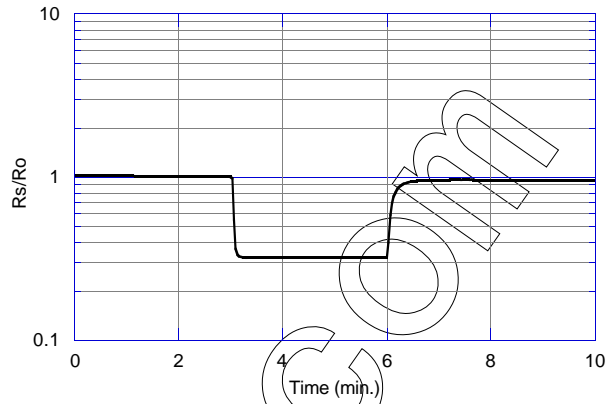


Fig. 11 - Gas response to hydrogen

Figure 12 shows the response pattern of the sensor when inserted into and later removed from 30ppm of ethanol after a 3 minute period. The Y-axis shows the ratio of sensor resistance over time ( $R_s$ ) compared with sensor resistance in clean air just prior to insertion into ethanol ( $R_o$ ).

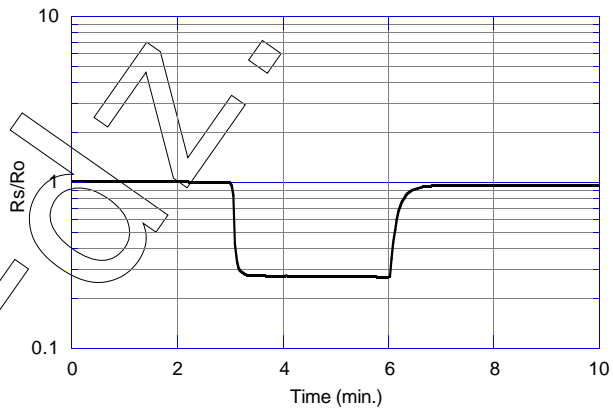


Fig. 12 - Gas response to ethanol

As these charts display, the sensor's response speed to the presence of gas is extremely quick, and when removed from gas, the sensor will recover back to its original value in a short period of time.

Figure 13 shows the response pattern of the sensor to the various gases found in cigarette smoke. The Y-axis shows the ratio of sensor resistance over time ( $R_s$ ) compared with sensor resistance after 1 minute in clean air ( $R_o$ ). This data was taken in a 20m<sup>3</sup> room with cigarettes placed on a flat surface. The burning time for one cigarette was approximately 8 minutes.

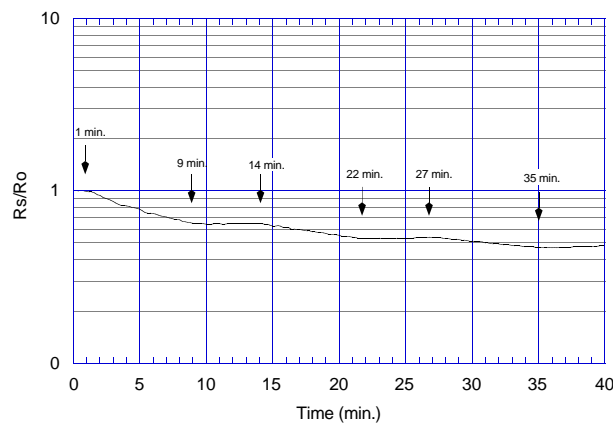


Fig. 13 - Response to cigarette smoke

This test consisted of the following sequence:

- 0- 1 min.: clean air (20°C/65%RH)
- 1- 9 min.: first cigarette burning
- 9-14 min.: no ventilation
- 14-22 min.: second cigarette burning
- 22-27 min.: no ventilation
- 27-35 min.: third cigarette burning

(Note: Generally, the activation point for an air cleaner would be around  $R_s/R_o=0.85$ , while the  $R_s/R_o$  for just one cigarette is as low as 0.65).

This data demonstrates that TGS2600 is ideal for usage in air cleaners designed to ventilate when cigarette smoke and other air contaminants are present.

2-5 Initial action

Figure 14 shows the initial action of the sensor resistance ( $R_s$ ) for a sensor which is stored unenergized in normal air for 30 days and then energized in clean air. The Y-axis represents sensor resistance in clean air at various times after energizing ( $R_s$ ) compared with sensor resistance 20 min. after energizing ( $R_o$ ).

The  $R_s$  drops sharply for the first seconds after energizing, regardless of the presence of gases, and then reaches a stable level according to the ambient atmosphere. Such behavior during the warm-up process is called "Initial Action".

Since this 'initial action' may cause an air cleaner to activate unnecessarily during the initial moments after powering on, it is recommended that an initial delay circuit be incorporated into the device's design (refer to ...).

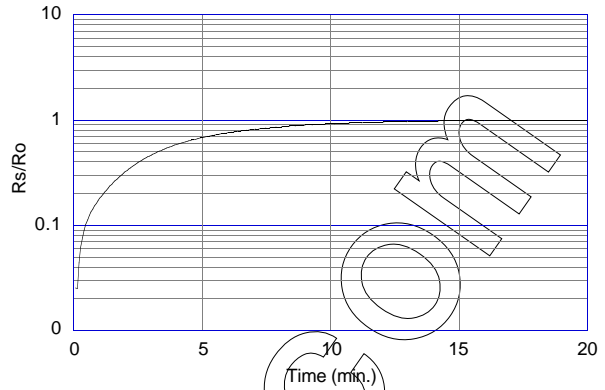


Fig. 14 - Initial action

2-6 Long-term characteristics

Figures 15 - 18 show the long-term stability of TGS2600 as measured for more than 400 days. In Figures 15 & 16, the sensor is first energized in normal air. Measurement for confirming sensor characteristics is conducted under standard test conditions. Figure 15 depicts sensor resistance in clean air over the test period, while in Figure 16 the Y-axis shows the ratio of sensor resistance in gases ( $R_s$ ) compared with sensor resistance in fresh air on the same day ( $R_o$ ).

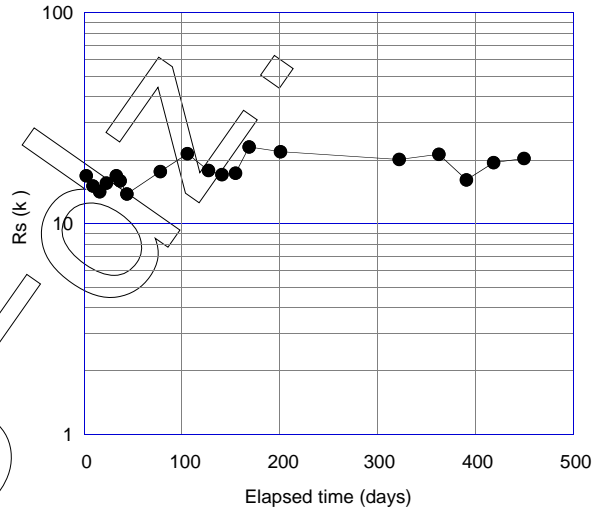


Fig. 15 - Long-term stability (continuous energizing) in clean air

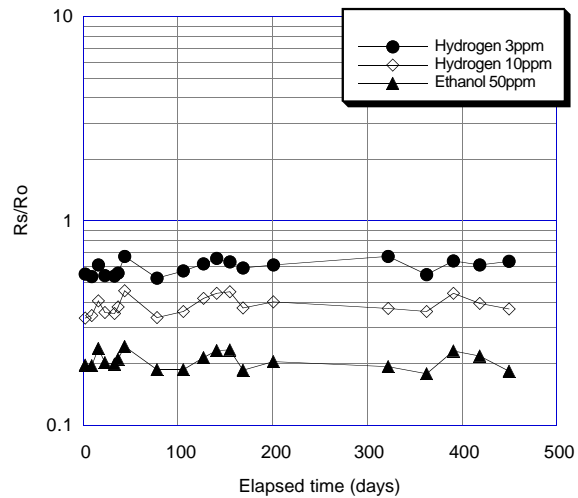


Fig. 16 - Long term stability (continuous energizing) in various gases



In Figures 17 & 18, the sensor is left unenergized in normal air for the entire test period except for the measurement period. Measurement for confirming sensor characteristics is conducted under standard test conditions. Figure 17 depicts sensor resistance in clean air over the test period, while in Figure 18 the Y-axis shows the ratio of sensor resistance in gases (Rs) compared with sensor resistance in fresh air on the same day (Ro).

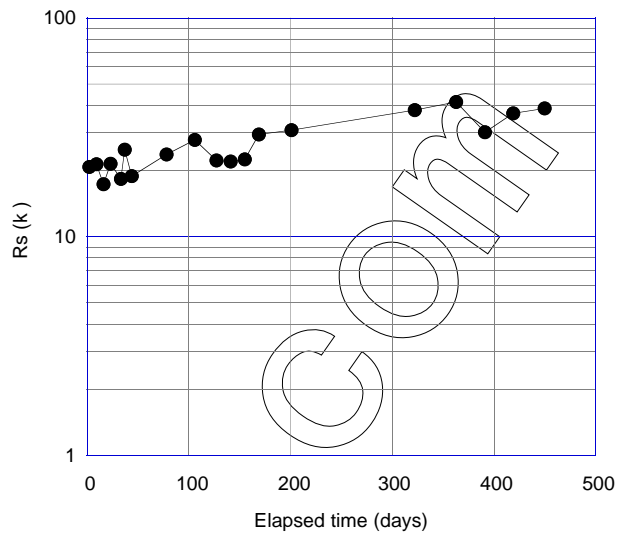


Fig. 17 - Long term stability (unenergized) in clean air

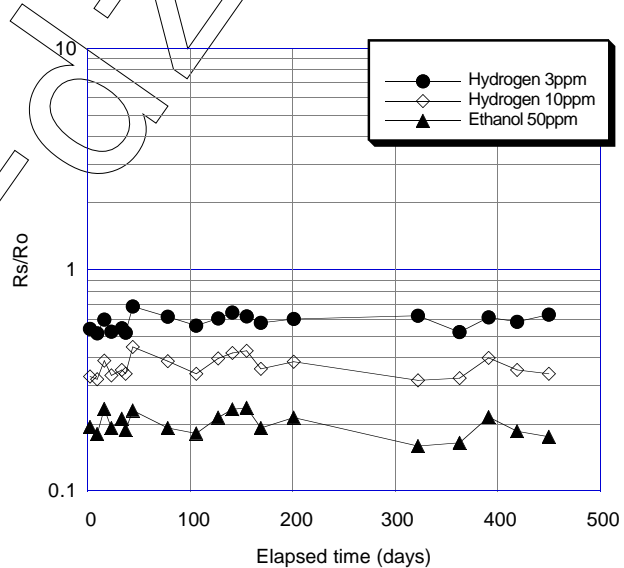


Fig. 18 - Long term stability (unenergized) in various gases

Figaro USA Inc. and the manufacturer, Figaro Engineering Inc. (together referred to as Figaro) reserve the right to make changes without notice to any products herein to improve reliability, functioning or design. Information contained in this document is believed to be reliable. However, Figaro does not assume any liability arising out of the application or use of any product or circuit described herein; neither does it convey any license under its patent rights, nor the rights of others.

Figaro's products are not authorized for use as critical components in life support applications wherein a failure or malfunction of the products may result in injury or threat to life.

**FIGARO GROUP**

**HEAD OFFICE**

**Figaro Engineering Inc.**  
 1-5-11 Senba-nishi  
 Mino, Osaka 562 JAPAN  
 Tel.: (81) 727-28-2561  
 Fax: (81) 727-28-0467  
 email: figaro@figaro.co.jp

**OVERSEAS**

**Figaro USA Inc.**  
 3703 West Lake Ave. Suite 203  
 Glenview, IL 60025 USA  
 Tel.: (1) 847-832-1701  
 Fax.: (1) 847-832-1705  
 email: figarousa@figarosensor.com

**Figaro Engineering Inc.  
 European Office**  
 Oststrasse 10  
 40211 Dusseldorf Germany  
 Tel: (49) 211-358807  
 Fax: (49) 211-359538